DESIGN SPECIFICATIONS FOR THE SECOND GENERATION SARCOS TREADPORT LOCOMOTION INTERFACE

John M. Hollerbach*
University of Utah
School of Computing
50 S. Central Campus Dr.
Salt Lake City, UT 84112
jmh@cs.utah.edu

Yangming Xu
Sarcos Research Corp.
360 Wakara Way
Salt Lake City, UT 84108
Yangming_Xu@ced.utah.edu

Robert R. Christensen
Evans & Sutherland Corp.
600 Kamas Dr.
Salt Lake City, UT 84108
robchris@es.com

Stephen C. Jacobsen
Sarcos Research Corp.
360 Wakara Way
Salt Lake City, UT 84108
Steve_Jacobsen@ced.utah.edu

ABSTRACT

The Sarcos Treadport is a locomotion interface comprised of a large tilting treadmill, an active mechanical tether, and a CAVE-like visual display. This paper presents the design specifications for the second-generation Sarcos Treadport.

INTRODUCTION

There have been various approaches towards the design of locomotion interfaces, including powered pedaling devices (Brogan et al., 1998), programmable foot platforms (Iwata, 2000), walking-in-place arrangments (Templeman et al., 1999), and treadmill-style devices. Of these alternatives, treadmills are particularly attractive because of the relatively natural, unencumbered walking and running that they allow.

Some treadmill-style devices employ linear treadmills which have been augmented in various ways, while other devices employ two-dimensional treadmill belt motion. The ATLAS system (Noma et al., 2000) comprises a linear treadmill on a spherical joint, which can act as a turntable but also tilt upwards and sideways. Turning is achieved by swiveling the treadmill in the direction of walking, based upon visual measurements of foot position. The Ground Surface Simulator (GSS) employs an array of 6 vertical motion stages underneath a flexible belt that deform the belt to create uneven terrain (Noma et al., 2000).

Turning is most naturally accomodated by two-dimensional treadmill designs. The Omnidirectional Treadmill employs orthogonal overlapping belts to create a two-dimensional surface (Darken et al., 1997). The top belt is comprised of rollers with rotation axes oriented parallel to the belt direction, and an orthogonal belt underneath moves the rollers to create motion at right angles to the top belt. Body position is measured by a mechanical tether. The Torus Treadmill employs an array of 12 small treadmills connected side-by-side to form one big belt, which is then rotated (Iwata and Yoshida, 1999). Magnetic trackers are employed to measure foot position and the intended direction of motion.

The Sarcos Treadport comprises a large tilting treadmill, an active mechanical tether attached to the user through a body harness, and a CAVE-like visual display. The six-axis mechanical tether measures body position and orientation, for the purpose of active control of treadmill belt speed and turning in the virtual world. Turning is achieved by rate control, indicated either by the amount of user yaw motion or the amount of sidestep, depending on user speed. Hence it is necessary for the user to reindex to center before turning the other way. The most unique aspect of the Treadport is that the tether's linear axis is motorized to push or pull on the user, thereby simulating unilateral constraints,

*Address all correspondence to this author.

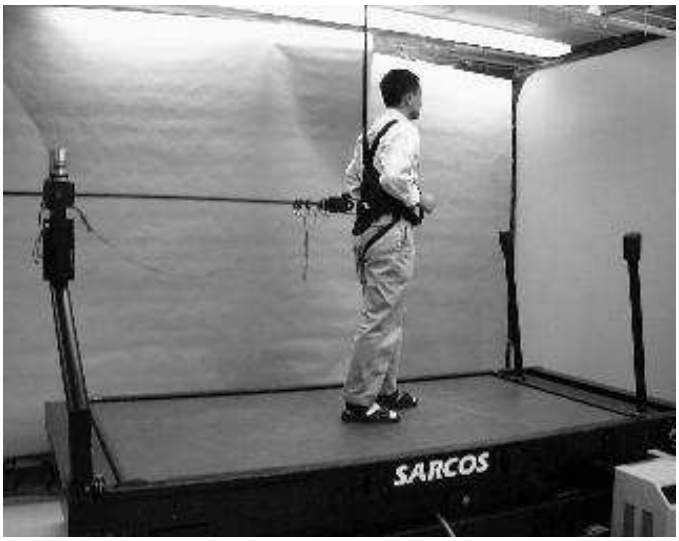

Figure 1. THE ORIGINAL SARCOS TREADPORT.

slope (Tristano et al., 2000), and inertial forces (Christensen et al., 2000).

The original Treadport (Figure 1) employed a commercial treadmill with a 4-by-8 foot belt area. Experience based on its use indicated that a larger belt area would be desirable for greater maneuverability, and that the tilt mechanism was too slow. The sensing of belt speed and tilt needed to be improved, as well as the force capability and responsiveness of the mechanical tether. Finally, we wished a larger and higher resolution CAVE display and the possibility of floor projection.

The new Sarcos Treadport is shown in Figure 2. The following sections discuss the design specifications for the treadmill belt, platform tilt, and the active mechanical tether. Safety mechanisms are also discussed, and the CAVE layout is briefly presented.

TREADMILL BELT

The belt area was increased to 6-by-10 feet, to provide greater forward and lateral maneuverability. To prevent belt jitter when a user stands still, a dead zone is created around the user's position in the center of the belt. There is also a safety zone near sides of the belt in which a user may not walk. The net result is that there is not much active space for sideways excursions of the user. In the forward direction, a greater belt distance would help avoid a situation of a fast user reaching the front edge of the belt. As discussed below, a larger running surface can also help to decrease the amount of tether force required in inertia display. A larger belt also will facilitate prone positions or crawling. To allow for the possibility of floor projection, it was decided to make the belt white.

The original Treadport employed a commercial treadmill

Figure 2. THE NEW SARCOS TREADPORT.

used for training runners. To best achieve the desired performance and sensing goals, it was decided that Sarcos should build its own treadmill for the second-generation Treadport.

The commercial treadmill of the original Treadport had a maximum velocity of 12 mph and a peak acceleration of 1 g. A literature survey showed that these velocity and acceleration capabilities were adequate for ordinary human runners, but not for competitive sprinters. Since the new treadmill is intended for ordinary users, we adopted the same specifications. To size the motor for the new Treadport, a simple model of the old Treadport system was created.

The load for the belt drive primarily arises from the belt friction against its backing and from the weight and impact of a user.

$$I\alpha = \tau_{belt} + \tau_{foot} + \tau_{motor} \tag{1}$$

where

I	is the inertia of the rollers, sprockets, belt, etc,
α	is the angular acceleration of the rollers,
τ_{belt}	is the torque due to friction when the treadmill belt runs without a user,
τ_{foot}	includes the friction from the normal force due to impact of the foot, as well as the braking force when the foot first strikes the belt, and
τ_{motor}	is the applied torque of the motor.

The load on the belt motor comprises the load due to the mechanism plus the load due to the user. For the belt mechanism, there is an inertial load $I\alpha$ due to the inertia of the rollers, belt, and drive mechanism. There is a frictional load τ_{belt} due to the belt sliding over its support surface or backing. For the original Treadport, the treadmill belt sliding on a waxed masonite backing was measured to have a coefficient of static friction of 0.23

Table 1. BELT DRIVE PARAMETERS EMPLOYED IN SIMULATION.

I (kg m^2)	inertia of rollers, etc.	0.07
r (m)	radius of motor	0.05
μ	coefficient of sliding friction	0.15
m_b (kg)	mass of belt	2.5
m_h (kg)	mass of human	90

and a coefficient of sliding friction of 0.15. The new Treadport employs the same backing.

During running, the user generates a load due to a braking force plus a friction force due to the normal impact force. Bobbert et al. (1991) used force plates to measure vertical ground reaction forces. A subject running at 5.3 m/s was found to have a peak reaction force of three times body weight which lasted for 0.2 seconds. Mero (1988) looked at the first foot contact after leaving the starting blocks in a sprint start. He measured a maximum horizontal braking force of 316 N, which lasted for 0.02 seconds. The friction force due to the normal force was added to the braking force. This number was then increased to six times the user's body weight to add some design margin to the estimate.

The impulsive load during running will cause some loss of belt speed, and one must decide how much slowdown is acceptable. We specified a maximum slowdown of 5% during running by a 90 kg user. Table 1 shows parameters that were employed in a simulation to determine motor sizing for the belt drive. The motor load is highly dominated by the impact forces from the running human. Figure 3 shows the simulation of running at 5 m/s with a 5 hp belt motor. The belt slowdown during impact was 4.6%, which satisfies the design specifications. For extra performance margin, a larger motor of 8 hp and 44.4 ft-lb peak torque was selected.

The diagram of the treadmill belt controller is shown in Figure 4. The user's position x_c relative to the treadmill center is measured by the tether. A PI controller yields a desired velocity of the belt v_{bd}. The proportional term drives the belt velocity while the integral term serves to recenter users and keep them from the front edge for safety purposes. The desired belt acceleration a_{bd} is determined from the velocity error from the actual belt velocity v_b, determined from belt position readings x_b. A feedforward controller that takes into account belt friction and inertia then drives the belt motor.

For the final system, a frequency response test showed a first-order model between desired and actual system. This model was incorporated into a Kalman filter for acceleration estimation, and the final controller shows good response.

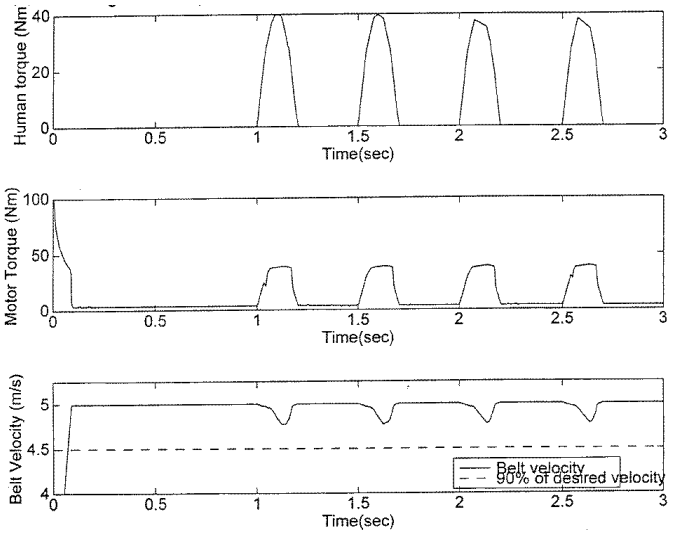

Figure 3. SIMULATION OF BELT VELOCITY VERSUS MOTOR TORQUE FOR A 5 HP MOTOR AND A 90 KG USER RUNNING AT 5 M/S.

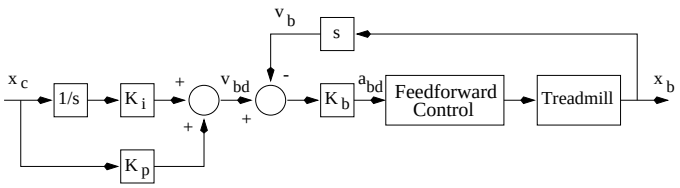

Figure 4. TREADMILL BELT CONTROLLER.

TREADMILL TILT

The original Treadport used the commercial Trackmaster TM-48 treadmill (www.trackmastertreadmills.com), which has a tilt capability of +14 to -5.7 degrees. The tilt mechanism was too slow to be useful, which was a primary reason to substitute tether force to display slope (Tristano et al., 2000). The tilt mechanism employed a lead screw drive at the front of the platform, which intruded into the field of view (Figure 1). There were different centers of rotation for the platform for upwards rotation from the horizontal versus downwards rotation from the horizontal. For downwards rotation, the center of rotation was at the middle of the belt, which is the desirable location. For upwards rotation, the platform rotates about a center at the back edge. This has the undesirable effect of lifting the user as well as elevating the slope. Finally, the platform did not come equipped with a tilt sensor.

It was decided that the ± 20 degrees of the original treadmill was adequate; Figure 5 shows this maximum tilt for the new Treadport. Somewhat arbitrarily, we chose that a 20 degree movement should be achieved in 1 second. This represents a kind of tradeoff between a reasonably fast tilt, safety, and excessive actuation demands. For fast slope transients, we can instead

Figure 5. THE TILT CAPABILITY OF THE NEW SARCOS TREADPORT.

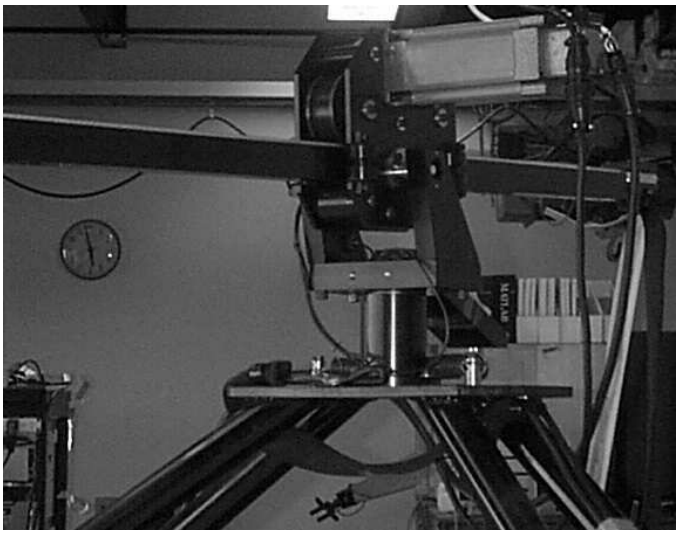

Figure 6. THE ACTIVE TETHER BASE JOINT.

rely on the active mechanical tether which are then blended in with the slower acting platform tilt. At the present time, the tilt mechanism on the new Treadport is not operational.

ACTIVE MECHANICAL TETHER

The active mechanical tether comprises a hook joint at the base, a sliding joint that connects the base to the user, and a spherical joint at the attachment point to the harness worn by the user. A rotary motor drives the sliding joint through a timing belt. The tether measures the full position and orientation of the user, and also exerts a force along the linear axis. The base joint of the new Treadport is shown in Figure 6.

Of the various purposes for an active mechanical tether, the display of inertial force is the most demanding. It has been found that users actually prefer a fractional amount of the inertia force,

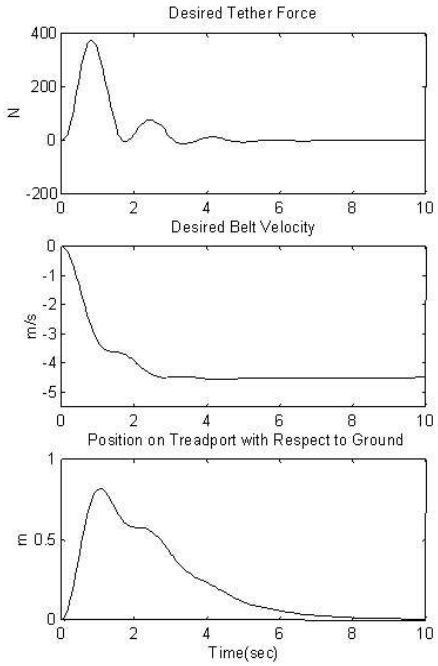

Figure 7. SIMULATION DURING SPRINTING FROM REST OF THE USER'S POSITION ON THE TREADMILL WITH RESPECT TO GROUND, THE BELT VELOCITY, AND THE REQUIRED TETHER FORCE FOR INERTIAL DISPLAY.

$f = 0.8 m_h a$, where m_h is the user's mass and a is the user's acceleration, perhaps due to the localized application of force to the body (Christensen et al., 2000). For a 90 kg user accelerating at 1 g, there would be a requirement for $f = 0.8 m_h g = 720$ N of tether force. Such a requirement raises serious safety issues and so is considered to be impractical. A mitigating factor is that some forward motion on the platform is allowable due to the 10-foot length. Therefore the user can experience some real acceleration, and so a lesser inertial force display will be required.

For the first generation Treadport, the tether force was limited to 190 N = 43 lb. The belt velocity was limited by the software to 5 m/s = 11 mph. For the purposes of design specification, the saturation of Treadport actuators was not considered in a simulation, created for the case of starting from rest and sprinting forward at maximum acceleration. The running model is based on an exponential equation described in (Christensen et al., 2000). The control algorithm for the tether and the belt were optimized to minimize the applied tether force. This was achieved by allowing the user to almost reach the end of the safe operating area at the front of the treadmill. Figure 7 shows the desired belt velocity and the resulting force required of the tether. The peak tether force is roughly 350 N = 78 lb. The figure also shows how the user has moved forward on the belt about 0.8 m.

For the old Treadport, it was found that even with the limits

on the tether force and belt velocity, the treadmill case matched closely with running on the ground (Christensen et al., 2000). Since the new Treadport is 10 feet long instead of 8 feet long, the user can be allowed to go further forward, so the required tether force can be reduced. It was decided to size the tether force at 315 N = 70 lb.

A power spectrum analysis of human sprint starts shows that the bandwidth is roughly 0.5 Hz, based on the use of Hill's equation (Christensen et al., 2000). This bandwidth is representative of the large amplitude signals from sprint starts, but for other motions the tether must be able to track the motion of each foot fall. Consequently we specified a 3 Hz bandwidth for such small amplitude signals.

In the case of simulating running into a wall, one could conceivably argue that the bandwidth should be much higher, as it would be required for a haptic interface simulating a hard surface. However, it appears that running into a hard wall is not something to be simulated with complete fidelity for reasons of comfort and safety.

Even with this tether force, there is a potential concern about a possible damaging load to the back. A survey of the biomechanics literature of the spine showed that a 70-lb load is well within normal load ranges and therefore does not pose a safety risk.

In the original Treadport, the kinematic arrangement of the tether is a spherical manipulator design, wherein there is a 2-axis Hookean joint at the base, an actuated sliding joint, and a spherical joint of pitch-yaw-roll design. Along the roll axis, which is the last axis, there is a linear offset between the harness attachment and the spherical joint center. This offset means that when a user is facing sideways a twisting torque is created by the tether. To reduce this lever effect, the spherical joint center on the new tether was placed flush against the user's back. This joint is a conventional roll-pitch-yaw design, in which the roll axis is now housed in the boom. There still exists a twisting torque when the user faces sideways, because the tether force cannot be directed through the center of the user's body. Designs were considered involving 4-bar linkages or circular tracks that would place the tether force through body center, but the added encumbrance and limitations on movement were not considered worth the benefit. The workspace of the base joints was also improved to allow greater maneuverabilty in the vicinity of the base.

The harness has leg loops, shoulder straps, and belts for the waist and chest. These straps are all adjustable for the individual user.

There is a force sensor at the attachment point of the tether end. Because of backlash in the attachment of the harness to the user, it was difficult to make closed-loop force control of the tether stable. Instead, we use open-loop force control. A much lower gear ratio is used on the new tether as compared to the old tether, so that the motor is more backdrivable and frictional losses are less. Tests determined a linear response between motor commands and tether force (Figure 8).

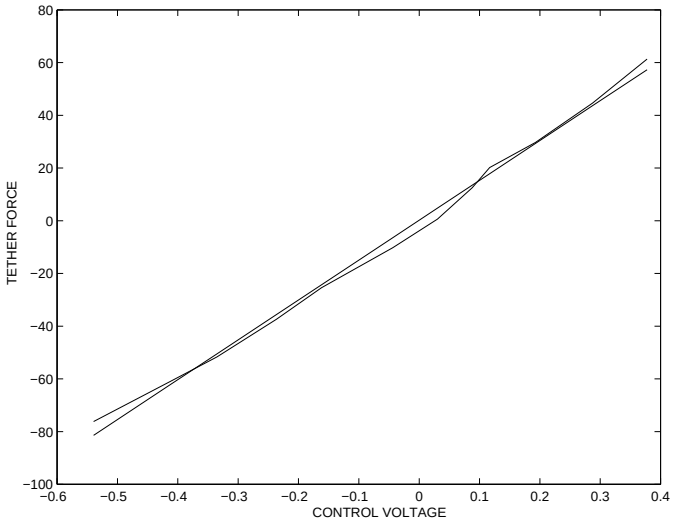

Figure 8. FORCE VERSUS VOLTAGE MOTOR COMMAND FOR THE TETHER.

SAFETY MECHANISMS

Because the human weight and the forces of running are to be accomodated, locomotion interfaces have to be large and capable of producing substantial forces. Safety can be a much more pressing concern than for haptic interfaces. Several mechanisms have been implemented to ensure user safety.

There are kill switches held both by the user and the operator. The user must depress and hold a switch in a hand-held unit for the treadmill to operate. There is a ceiling restraint attached to the harness worn by the user, which operates like a car seat belt. A lock is triggered when there is a sudden jerking of the ceiling tether, which catches a user who is falling. There are mechanical limit stops on the linear axis of the tether. There is also a watchdog timer for the computer.

Kinesthetic cues are also provided as an aid to staying centered on the treadmill belt. The tether force is made spring-like, which pulls the user back to the belt center. On the yaw joints at the base and at the harness attachments, there are torsional springs which resist a user turn to the left or right. These spring resistances provide kinesthetic information about the center position on the belt. An integral control term in the Treadport controller also recenters the user on the belt at any steady state velocity (Christensen et al., 2000).

Various position, motion, and force limits are enforced by software. There is a bounding box for safe operation that prevents excursions too close to the sides, front, and back, as well as apparent motions too high or too low to the belt. Gradual ramp up during startup is enforced for belt velocity and tether

force. Limits are placed on the speed of backward motion.

CAVE DISPLAY

Figure 2 shows the CAVE (Cruz-Neira et al., 1993) display for the new Treadport. Three screens are placed in a flared arrangement, with the side screens rotated 60 degrees from the front screen. The flaring gives a rough approximation to a cylindrical display. The screens are highly diffuse acrylic back-projection screens. Three Hughes-JVC G1000 SXGA projectors create the graphical images. Mylar mirrors fold the optical path to preserve space.

COMPUTER ARCHITECTURE

The Treadport is controlled by a VME-based microprocessor system. The real-time operating system VxWorks (Wind Rivers Inc.) is employed on a Motorola PowerPC 604e board, and the ControlShell component-based programming language (Real Time Innovations, Inc.) is employed to encode the controller. An SGI 4-processor, 2 graphics-head Onyx is employed to create the graphical images.

DISCUSSION

This paper has presented the second-generation Treadport and the design specifications in its creation. Current research focuses on mechanical issues of turning control methods and irregular slope display, and visual issues of display cues for depth perception (Hollerbach et al., 1999).

ACKNOWLEDGMENT

This research was supported by ONR Grant N00014-97-1-0355, by NSF Grant IIS-9908675, by NSF Grant CDA-96-2361, and by an NSF Graduate Research Fellowship. We thank Rod Freier for his contributions on the computer architecture and controller. Martin Buehler kindly offered information about design considerations for his treadmill design. Pete Shirley and Bill Thompson were responsible for the CAVE. Sandy Meek assisted with the spine biomechanics literature. We thank Sarcos engineers for the detailed design and fabrication.

REFERENCES

Bobbert, M.F., Schamhardt, H.C., and Nigg, B.M., "Calculation of vertical ground reaction force estimates during running from positional data," *J. Biomechanics, 24,* 1991, pp. 1095-1105

Brogan, D.C., Metoyer, R.A., and Hodgins, J.K., "Dynamically simulated characters in virtual environments," *IEEE Computer Graphics and Applications, 15,* 1998, pp. 58-69.

Christensen, R., Hollerbach, J.M., Xu, Y., and Meek, S., "Inertial force feedback for the Treadport locomotion interface," *Presence: Teleoperators and Virtual Environments, 9,* 2000, pp. 1-14.

Cruz-Neira, C., Sandin, D., and DeFanti, T.A., "Surround-screen projection-based virtual reality: the design and implementation of the CAVE," *ACM SIGGRAPH'93 Proceedings,* Anaheim, CA, Aug. 1993, pp. 135-142.

Darken, R.P., Cockayne, W.R., and Carmein, D., "The Omni-Directional Treadmill: A Locomotion Device for Virtual Worlds," *Proc. UIST,* 1997, pp. 213-221.

Hollerbach, J.M., Thompson, W.B., and Shirley, P., "The convergence of robotics, vision, and computer graphics for user information," *Intl. J. Robotics Research, 18,* 1999, pp. 1088-1100.

Iwata, H., "Locomotion interface for virtual environments," *Robotics Research: the Ninth International Symposium,* J. Hollerbach and D. Koditschek, eds., Springer-Verlag, London, 2000, pp. 275-282.

Iwata, H., and Yoshida, Y., "Path reproduction tests using a Torus Treadmill," *Presence: Teleoperators and Virtual Environments, 8,* 1999, pp. 587-597.

Mero, A., "Force-time characteristics and running velocity of male sprinters during the acceleration phase of sprinting," *Research Quarterly, 59(2),* 1988, pp. 94-98.

Moghaddam, M., and Buehler, M., "Control of virtual motion systems," *Proc. IEEE/RSJ Conf. Intelligent Robots and Systems,* Yokohama, 1993, pp. 63-67.

Noma, H., Sugihara, T., and Miyasato, T., "Development of ground surface simulator for tel-E-merge system," *Proc. IEEE Virtual Reality 2000,* New Brunswick, NJ, March 18-22, 2000, pp. 217-224.

Templeman, J.N., Denbrook, P.S., and Sibert, L.E., "Maintaining spatial orientation during travel in an immersive virtual environment," *Presence, 8,* 1999, pp. 598-617.

Tristano, D., Hollerbach, J.M., and Christensen, R., "Slope display on a locomotion interface," *Experimental Robotics VI,* P. Corke and J. Trevelyan, eds., Springer-Verlag London, 2000, pp. 193-201.